


RESEARCH ARTICLE

Long-term trends in wetland event response with permafrost thaw-induced landscape transition and hummock development

Kristine M. Haynes  | Ian Frederick | Brenden Disher | Olivia Carpino | William L. Quinton

Cold Regions Research Centre, Wilfrid Laurier University, Waterloo, Ontario, Canada

Correspondence

Kristine M. Haynes, Cold Regions Research Centre, Wilfrid Laurier University, 75 University Ave W, Waterloo, Ontario N2L 3C5, Canada.

Email: khaynes@wlu.ca

Present address

Brenden Disher, Environment and Climate Change Canada, Saskatoon, Saskatchewan, Canada.

Funding information

ArcticNet; Natural Sciences and Engineering Research Council of Canada

Abstract

Northwestern Canada's discontinuous permafrost landscape is transitioning rapidly due to permafrost thaw, with the conversion of elevated, forested peat plateaus to low-lying, treeless wetlands. Increasing hydrological connectivity leads to partial drainage of previously isolated wetlands, which subsequently develop hummock-hollow microtopography. Ultimately, the ecohydrological feedbacks associated with climate-driven permafrost thaw have led to the expansion of treed wetlands in plateau-wetland complexes. Field research and aerial imagery analyses were conducted at the Scotty Creek Research Station, Northwest Territories, to examine the development of hummock terrain over time and the resultant impacts on the hydrological response of wetlands connected to the basin drainage network. The area of peat plateaus underlain by permafrost declined between 2010 and 2018. The total area of hummock terrain increased in the basin in the same time period, with an overall decrease in the hummock perimeter-to-area ratio as small individual hummocks increased in size and aggregated into larger hummock complexes occupied by re-establishing trees. With the development and expansion of hummock terrain, the tortuosity of flowpaths draining wetlands increased. The average wetland water level recession constants following precipitation events became shorter over the 15 year period of record (2003–2017). The average time of water level rise in response to precipitation events decreased over time, as precipitation was directed quickly to runoff. As permafrost thaw reduces the cover of peat plateaus in exchange for increased wetland area, the presence of treed wetlands appears to be transitioning plateau-wetland complexes into permafrost-free forest, facilitated by the growth of hummock terrain. Permafrost thaw-induced wetland transition triggers ecohydrological feedbacks with the potential to alter the availability and sustainability of freshwater resources.

KEYWORDS

landscape change, microtopography, rainfall response, recession coefficient, transition wetlands

1 | INTRODUCTION

Northwestern Canada's subarctic region of plateau-wetland complexes in the sporadic to discontinuous permafrost zone is experiencing rapid permafrost loss as a result of climate change (Richter-Menge et al., 2017). Permafrost degradation and loss is catalysing dramatic landscape transition in this peatland-dominated region (Chasmer & Hopkinson, 2017; Jorgenson & Osterkamp, 2005; Lara et al., 2016; Quinton et al., 2019). Peat plateaus are underlain by ice-rich permafrost and are topographically elevated by approximately 0.5 to 1.5 m (Wright et al., 2009) above permafrost-free wetlands including channel fens and collapse scars. Peat plateaus shed water efficiently to these low-lying wetlands given the pronounced hydraulic gradient (Chasmer et al., 2014; Hayashi et al., 2004; Quinton et al., 2011). A canopy dominated by black spruce is rooted in peat plateaus, as this landform type maintains sufficiently low soil moistures to support these tree species in an otherwise saturated landscape (Islam & Macdonald, 2004). Permafrost thaw destabilizes peat plateaus resulting in the subsidence of their ground surfaces. As degraded plateaus are inundated by adjacent wetlands, their tree canopies are lost and such plateaus transform into collapse scar wetlands, which are treeless, permafrost-free and low-lying water stores or conveyances (Quinton et al., 2011).

Permafrost thaw and the resultant landscape transition initiate significant ecohydrological feedbacks in northern peatlands (Waddington et al., 2015), which impact the storage and routing of water. Isolated wetlands store water received from precipitation and from 'primary runoff', defined by Connon et al. (2014) as direct runoff from adjacent plateaus. As permafrost below the plateaus that separate wetlands begins to thaw, such previously separated wetlands develop hydrological connections over intervening areas of subsided peat plateau. Over time, this process connects hydrologically isolated wetlands to the basin drainage network through the process of 'wetland capture' (Connon et al., 2014). As the permafrost that once kept isolated wetlands from shedding water degrades, 'captured' wetlands are able to partially drain through the new hydrological connections leading to the broad, linear channel fens that convey precipitation and drainage, and contribute a portion of their previously stored water to the basin hydrograph (Haynes et al., 2018). Basins in the Northwest Territories subjected to widespread permafrost thaw have demonstrated significant increases in mean annual discharge over multi-decadal records (St. Jacques & Sauchyn, 2009). In the Scotty Creek basin of the lower Liard River valley, the increasing proportion of the landscape that is hydrologically connected to the basin outlet was the primary driver of increasing basin discharge, with other drivers, including increased precipitation, water from melting ice within permafrost and increasing groundwater as evidenced by increasing baseflow, all making relatively minor contributions (Connon et al., 2014). As previously isolated wetlands developed hydrological connections to adjacent wetlands and ultimately to the channel fen drainage network, the loss of water from wetland storage contributed to the rising rates of basin runoff in the increasingly interconnected landscape (Haynes et al., 2018). Moreover, examination of composite hydrographs for

basins in the lower Liard River valley demonstrated a shift in the timing of discharge as the landscape has changed with permafrost thaw (Quinton et al., 2019). For example, in the 1976 to 1985 decade, while rates of permafrost thaw were relatively low, Quinton et al. (2019) showed that the spring freshet dominated annual hydrographs. In subsequent, warmer decades when permafrost thaw was more advanced and as a result, the landscape more hydrologically connected, the cumulative annual discharge from basins increased significantly (Connon et al., 2014; St. Jacques & Sauchyn, 2009), with greater discharge during the freshet and the emergence of a secondary peak in late summer indicating greater rainfall-driven discharge (Quinton et al., 2019). Recession flow analysis has been used in permafrost environments to assess the rate of permafrost thaw based on long-term streamflow records, including in the Yukon River basin (Lyon et al., 2009; Lyon & Destouni, 2010). Such an analysis has not been applied to assess the impacts of landscape change on the response of wetland water levels to precipitation events as an approach to better understand the ecohydrological feedbacks with wetland transition.

Permafrost thaw alters vegetation communities and successional trajectories and increases peat accumulation (Camill, 1999a, 1999b). The partial drainage of newly-connected wetlands initiates an ecohydrological feedback process, which, through a number of stages over several decades, transforms a collapse scar wetland to treed wetland without any permafrost regeneration (Carpino et al., 2021). As collapse scar wetlands dewater, the net primary productivity of drought-tolerant vegetation, including *Sphagnum* species that colonize hummocks, increases and as such, mature collapse scar wetlands support well-developed hummock-hollow microtopography (Haynes et al., 2020). The transition of open, flat collapse scar wetlands to treed wetlands is facilitated by the ecohydrological feedbacks initiated by permafrost thaw (Disher et al., 2021) and driven by the development of hummock terrain (Haynes et al., 2020). The development of treed wetlands is enabled by the elevated hummock surfaces that are sufficiently dry to support the growth of black spruce (Islam & Macdonald, 2004) as well as tamarack. The changing hydrology of the transitioning landscape is evident from the ecological and physical changes triggered by permafrost thaw. However, the subsequent ecohydrological impacts of hummock development and expansion of wetland drainage connections on the routing of water through the transitioning landscape, water level response to rainfall and subsequent recession remain poorly understood.

The overarching objective of this study is to develop a better understanding of the ecohydrological feedbacks associated with permafrost thaw-induced wetland transition, in particular hummock development, in the Taiga Plains. This will be accomplished through the following specific objectives: (i) assess changes in wetland water level response to precipitation from 2003 to 2017, a period of rapid landscape transition that corresponds to the period of water level measurement; (ii) compare the landscapes as they appeared in 2010 and 2018 as a means to evaluate how permafrost thaw-induced changes have altered the relative occurrence of landform types in the Scotty Creek basin; and (iii) track the change in the area occupied by hummock terrain, as well as the physical characteristics of individual

hummocks, and quantify potential changes between 2010 and 2018 in the tortuosity of flowpaths within wetlands connected to the basin drainage network.

2 | STUDY SITE

Within the sporadic-discontinuous permafrost zone, the Scotty Creek Research Station (61.44°N, 121.25°W) is located approximately 50 km south of Fort Simpson, Northwest Territories (Figure 1). Mean annual air temperature (MAAT) at Fort Simpson has increased from -4.1°C (1960–1980) to -2.9°C (1981–2010). The most pronounced increases in air temperature have occurred during the winter months, with an increase of 3.4°C in mean January temperatures from 1960–1980 (-28.0°C) to 1981–2010 (-24.6°C). Mean July temperatures have increased 0.6°C from 1960–1980 (16.8°C) to 1981–2010 (17.4°C). Mean annual precipitation in 1960–1980 was 347 mm with 42% (145 mm) falling as snow, while mean annual precipitation for the period of 1981–2010 was 390 mm with 38% (149 mm) falling as

snow. The portion of the Scotty Creek watershed gauged by the Water Survey of Canada covers approximately 152 km^2 (Quinton et al., 2003; Quinton & Baltzer, 2013). It is composed of heterogeneous, permafrost-free upland moraines predominantly in the northern portion of the basin, while the headwaters region (the focus of this study) is dominated by raised permafrost plateaus, collapse scar wetlands, channel fens and lakes (Chasmer et al., 2014). The elevated peat plateaus underlain by permafrost are forested with a canopy of black spruce (*Picea mariana*) trees with an understory of ericaceous shrubs (e.g., *Rhododendron groenlandicum*), lichens (*Cladonia* spp.) and mosses (*Sphagnum* spp.). Given the relatively warm temperature of permafrost (near 0°C) in this area (Jorgenson et al., 2001), the landscape is vulnerable to permafrost thaw-induced change (Carpino et al., 2021; Quinton et al., 2011). As permafrost thaws, the ground surface subsides and becomes inundated by adjacent wetlands, resulting in the loss of tree cover and the expansion of open collapse scar wetlands. These wetlands are vegetated with ericaceous shrubs including leatherleaf (*Chamaedaphne calyculata*), bog rosemary (*Andromeda polifolia*) and small cranberry (*Vaccinium oxycoccos*)

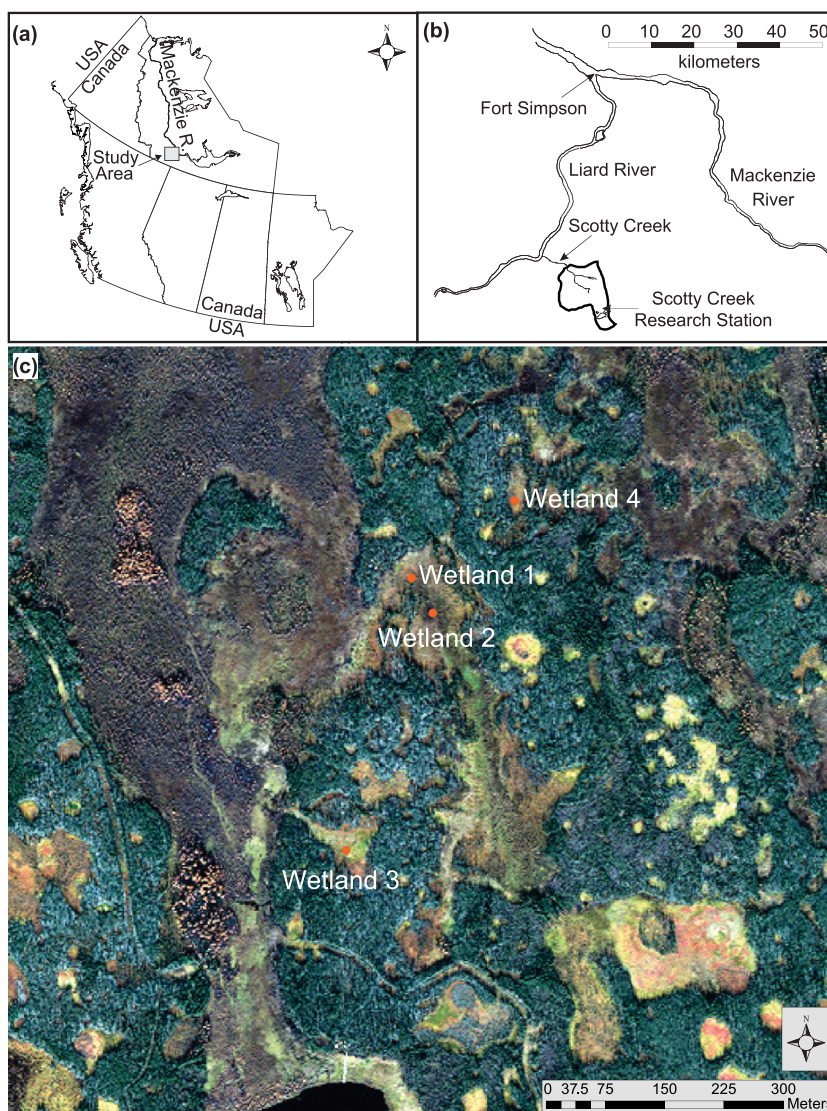


FIGURE 1 (a) Location of the study area in the Northwest Territories (NWT), Canada; (b) location of the Scotty Creek Research Station in the lower Liard River valley, 50 km south of Fort Simpson, NWT; and (c) locations of the long-term monitoring water level wells (orange dots) in each of the four monitored connected wetlands (Wetlands 1–4)

(Garon-Labrecque et al., 2015). The dominant bryophyte species in the wetlands include *Sphagnum balticum* and *Sphagnum magellanicum* (Garon-Labrecque et al., 2015) as well as *Sphagnum riparium* particularly in the wettest sites including recent permafrost thaw-induced collapse scar wetlands (Gibson et al., 2018; Pelletier et al., 2017). Drying of wetlands resulting from permafrost thaw and wetland 'capture' (Connon et al., 2014; Haynes et al., 2018) promotes the colonization of *Sphagnum* species that tolerate drier conditions, including *Sphagnum fuscum*, in the form of hummocks (Haynes et al., 2020). These hummocks facilitate the establishment and growth of trees, including black spruce (*P. mariana*) and tamarack (*Larix laricina*), resulting in the formation of hydrologically distinct treed wetlands (Disher et al., 2021). Channel fens in this basin are dominated by floating vegetative mats of predominantly sedges (*Carex* and *Eriophorum*) with tamarack (*L. laricina*) and birch (*Betula glandulosa*) trees scattered throughout the fens (Garon-Labrecque et al., 2015). Peat deposits in the Scotty Creek watershed range from 2 to 8 m in depth (McClymont et al., 2013).

3 | METHODS

3.1 | Wetland water level measurements

Water levels were monitored beginning in 2003 in four wetlands that have become connected to the basin drainage network over time as the landscape changes (Figure 1c). Wetlands 1 and 2 developed connections to the drainage network just before 1970, while Wetland 3 became connected in the 1980s or 1990s (between 1977 and 2000 aerial imagery; Quinton et al., 2011). Within the last decade, Wetland 4 has developed a connection to an adjacent wetland to the east and likely forms part of a wetland cascade draining into the channel fen to the east of Wetland 4. A pressure transducer installed in a 5 cm diameter, PVC slotted well was used to monitor the water level in each wetland. From 2003 to 2012, vented pressure transducers (Global Water WL15x and WL16s, Gold River, CA, USA) were used. In 2013, the vented transducers were replaced with transducers measuring total (i.e., atmospheric plus water) pressure (Levellogger Gold F15/M5, Solinst Canada Ltd., Georgetown, ON, Canada, and HOBO U20 Water Level Data Logger, Onset Computer Corporation, Bourne, MA, USA). A barometric pressure transducer (Solinst Barologger Gold) installed in the study area was used to correct the well data for barometric pressure. Water level measurements were recorded at 30 min intervals. Over the period of 2003 to 2013, water level loggers were installed in the wells each year either during or immediately following the spring snowmelt and removed prior to freeze-up towards the end of the growing season in the late summer or early fall. Beginning in 2014 for Wetland 1 and in 2015 for the other three wetland wells (Wetlands 2–4), the pressure transducers were lowered approximately 1.5 to 2 m within each well at the end of the growing season to prevent freezing and remained in the wells over the winter season.

In order to compare the water level trends in both hummocks and inter-hummock hollows, one slotted stilling well was installed through

a hummock (referred to as 'hummock' throughout) and one in a low-lying inter-hummock hollow (referred to as 'hollow') at the end of the 2019 growing season. These two wells were installed in a treed wetland, which has developed over time from a collapse scar wetland that formed as a result of permafrost thaw-induced peat plateau subsidence. The hydraulic gradient between these two wells was examined over the 2020 growing season to assess the flow dynamics between elevated hummocks and low-lying inter-hummock hollows.

To convert the pressure transducer measurements to actual water level depths, manual measurements from the top of the well casing to the water level recorded at both sensor installation and removal were used. Absolute elevation (in metres above sea level [m asl]) for the top of each well casing was measured using a differential global positioning system (dGPS; SR530 RTK, Leica Geosystems Inc., Norcross, GA, USA; system accuracy ± 0.02 m), facilitating the expression of the water level positions with a common datum.

3.2 | Wetland water level responses to precipitation

Examining the characteristics of the relationship between precipitation and runoff generation is typically performed manually and is therefore often subjective in event identification as well as time consuming, particularly with long-term records (Tang & Carey, 2017). In an effort to ensure consistency and efficiency in hydrograph-hydrograph analyses, Tang and Carey (2017) developed a MATLAB-based toolbox called HydRun, which is a flexible analysis package that can be parameterized to determine the time characteristics for rainfall-runoff events.

To examine the characteristics of event-based wetland water level responses for the four monitored wetlands, HydRun (Tang & Carey, 2017) was applied. For our study, HydRun was adapted through parameterization to understand the changing wetland water level response to precipitation events in connected wetlands over time as the discontinuous permafrost landscape changes. For the purpose of water level response analyses, HydRun was applied using the 'Baseflow-free' setting and the user-defined parameters for extracting event responses (peak threshold, return threshold/ratio, etc.) were systematically altered to optimize the selection of growing season precipitation events and wetland water level responses. As defined by Tang and Carey (2017), the return threshold or ratio is the difference between the flows at the start and end of an event to set the local minima, while the peak threshold allows for the filtering out of small fluctuations to analyse events above a predefined value. Annual water level records (with 30 min time steps) for the four monitored wetlands with long-term measurements were examined using HydRun in conjunction with precipitation measurements (30 min intervals) collected using a Geonor T-200B weighing precipitation gauge equipped with alter shield.

Three mean annual water level response parameters in the output of the HydRun analyses were examined for growing season rainfall events in the four wetlands over the period of 2005–2017. Events

with a normalized root-mean-square error (NRMSE) of ≤ 0.1 were selected for further analysis of the resultant event response parameters. Mean annual recession coefficients were examined to assess potential changes in recession characteristics over time with landscape change. Mean annual time of rise (time between the beginning of the event response and the peak water level) and centroid lag (time between centroid of effective precipitation and centroid of event water level response) were tracked over time to examine potential changes in the response of wetlands to precipitation events.

3.3 | Landform classification

To examine the change in areal extent of the landform types that comprise the Scotty Creek basin, landform classifications were performed in both 2010 and 2018 within an approximately 17 km² area of the peatland-dominated headwaters portion of the basin. For both the 2010 and 2018 landscapes, a supervised image classification using a support vector machine (SVM) algorithm was completed. To accurately identify all landforms, including different landform types with tree canopies (peat plateaus and treed wetlands), the classifications were performed using a fusion approach with WorldView 8-band multispectral imagery (WorldView-2 for 2010 and WorldView-3 for 2018) and an object-based analysis of Light Detection and Ranging (LiDAR) data, and its subsequent derived products including a digital elevation model (DEM), canopy height model (CHM) and canopy gap fraction model (used only for 2010, as not available for 2018). The WorldView-2 imagery was collected at a resolution of 2 m, while the WorldView-3 imagery was collected at a resolution of 0.5 m. The LiDAR data used in these classifications were collected over the Scotty Creek basin at a resolution of 1 m (see Chasmer et al., 2011, for LiDAR processing details). These data were resampled and aggregated to provide a consistent working resolution of 2 m.

Given the difficulty in differentiating between low-elevation landform types with sporadic tree canopy cover, such as treed wetlands and channel fens, the classification of these features relied upon both spectral and topographic properties. The classification of the upland, although minimal in the headwaters portion of the Scotty Creek basin, was conducted using canopy characteristics (i.e., CHM and canopy gap fraction products). Uplands were only classified for 2010, and the 2010 upland classification was used for the 2018 classification, as it is assumed that these permafrost-free features are relatively stable over time compared to the surrounding peatland landscapes.

Training sites for each of the landform types were selected to perform the supervised classifications. These validation sites were selected from multispectral aerial imagery, including sites validated by field work. For each of the peat plateau, channel fen and collapse scar wetland landform types, 25 training sites were chosen. For the treed wetland class in both the 2010 and 2018 classifications, 10 training sites were selected for the accuracy analysis. Given the unbalanced number of training sites for each of the landform types being classified, the SVM approach was chosen as the optimal classification technique.

To reduce potential discrepancies within both the 2010 and 2018 classifications, open water present within the area of interest was masked out of the final imagery. A low-pass filter (3×3) was used to minimize noise and 'speckle' of the classified spectral products. The boundary clean tool was used on the final classified products (i.e., after the spectral and object-based classifications were merged into the final classification). The topographic position index (TPI), which uses neighbourhood-based focal statistics to assess the mean elevation within a specified area, was used to de-trend the DEM and identify topographically-elevated features. A circular neighbourhood (with a diameter of 125 m) was deemed most appropriate to discern high- and low-elevation features. For each landform type, appropriate thresholds for the TPI and CHM were determined.

3.4 | Identifying hummocks and their physical characteristics

In the 0.6 km² area of the Scotty Creek headwaters where the long-term wetland sites were monitored, the distribution of hummocks was identified and their physical characteristics were compared between 2010 and 2018 through the use of high-resolution imagery. As described in Haynes et al. (2020), the spectral differences (predominantly colour) between *Sphagnum* species that occupy different positions in the landscape (i.e., *S. fuscum* of hummocks as compared to aquatic *S. riparium*) facilitate the identification of hummocks.

For the determination of hummock terrain in the 2010 and 2018 landscapes, an unsupervised principal component analysis (PCA) classification was performed on the WorldView-2 and WorldView-3 imagery, respectively, using the ArcGIS suite of products. Five components were identified in each of the classifications, one of which represented the targeted hummock-dominated terrain. This product was then reclassified into three classes to estimate the wetland area with and without hummocks and also classified the remaining landform types (e.g., peat plateau, channel fen and mineral upland) as 'other'. The 'other' category was isolated and removed from the classified product leaving a binary raster (i.e., with or without hummock terrain) that overlaid and corresponded with the boundaries identified in the landform classification of collapse scar and treed wetlands. The 2018 hummock classification using the multispectral imagery was combined with a high-resolution digital terrain model (DTM) created using a Remotely Piloted Aircraft System (RPAS), as described in Haynes et al. (2020). As a DTM was not available for 2010, hummock identification was completed based only on the multispectral WorldView-2 imagery. Comparison of the 2018 spectral and DTM-based surface slope approaches revealed a high degree of agreement (>90%). Therefore, the purely multispectral approach for the 2010 landscape was deemed suitable.

Using the 2010 and 2018 hummock classifications, hummock characteristics were compared between the 2 years. Total hummock area (expressed in m² and as a percentage of the 0.6 km² studied area), hummock perimeter and the perimeter-to-area ratios were assessed using the Zonal Geometry tool in ArcGIS for both 2010 and 2018. In

this analysis, total hummock area and perimeter, as well as the perimeter-to-area ratios calculated from these measurements, refer to the combined area and perimeter of all individual hummocks identified within the 0.6 km² study area. In addition to the overall 0.6 km² study area, these metrics were also determined individually for the four wetlands that were monitored for long-term water level measurements.

3.5 | Flowpath tortuosity

A particle tracking technique, following the method of Quinton and Marsh (1998), was used to estimate the tortuosity of flowpaths draining the connected wetlands in both 2010 and 2018. The tortuosity (T_x) of hydrological flowpaths was determined based on the following equation:

$$T_x = \frac{L_F}{L_S}$$

which is the ratio of the length of the flowpath (L_F) followed by water from a point in a wetland to the length of a straight line (L_S) with the same starting and ending points. Particle tracking runs were repeated

50 times for each of the four wetlands, and the average flowpath tortuosity was determined for each site. Using ArcGIS, 50 random points were generated within each wetland as starting points for hydrological flowpaths. From these points, the cost distance (L_F), using hummocks as barriers to flow, and the straight-line distance (L_S) to the wetland outlet were determined in both 2010 and 2018.

4 | RESULTS

4.1 | Water level response characteristics

Recession constants of water level responses to precipitation events in the monitored wetlands became shorter over the period of record (Figure 2a, i). The average recession constant was 48 ± 4 h in 2005, which decreased to 27 ± 10 h in 2017. Water level recession constants normalized by total annual precipitation also exhibited a decline over the period of record (Figure 2a, ii), indicating that the shortening of recession constants over time was not likely a function of inter-annual variation in total precipitation amounts.

Similar to the recession constants, the time of rise of the wetland water levels in response to precipitation events decreased over the

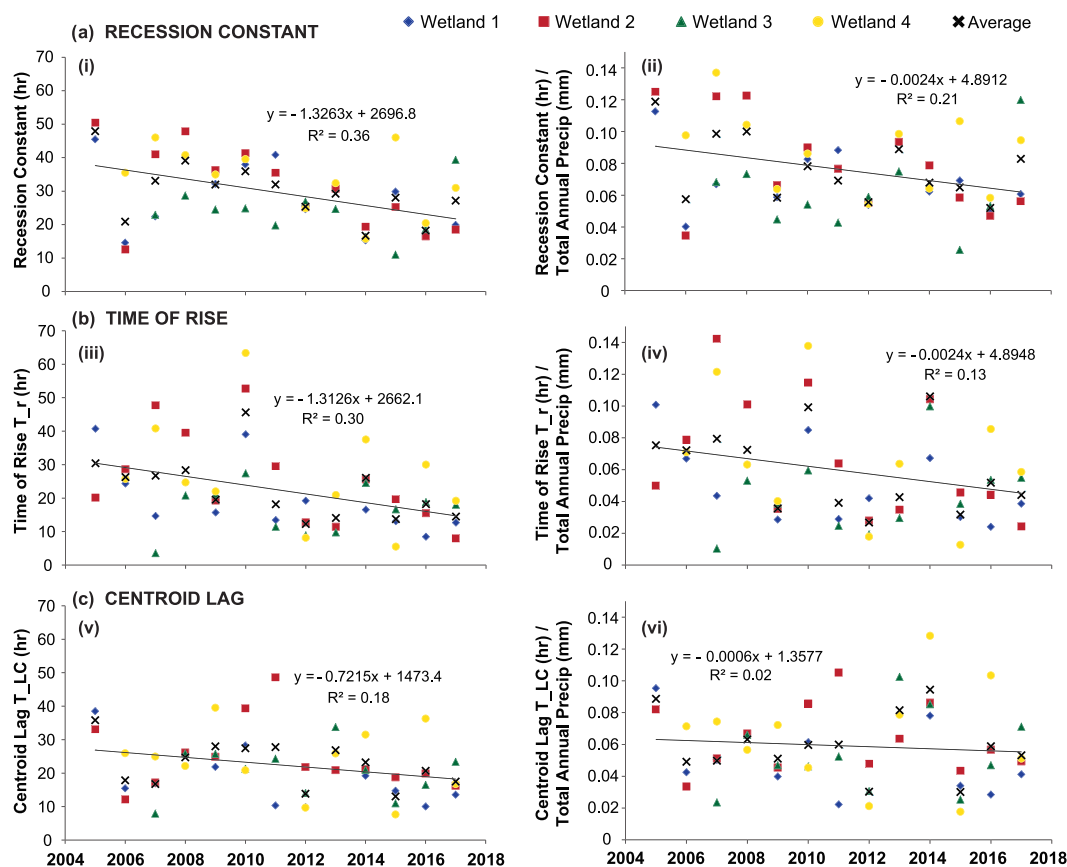


FIGURE 2 Average annual (a) recession constants (i, ii), (b) time of rise (iii, iv) and (c) centroid lag (v, vi) parameters for each of the monitored wetlands as well as the average of the wetlands over the period of 2005 to 2017. Parameters normalized by total annual precipitation are presented in panes (ii), (iv) and (vi) for recession constants, time of rise and centroid lag, respectively, to illustrate the effect of annual precipitation on the mean event response of the connected wetlands.

period of study (Figure 2b, iii). When normalized by total annual precipitation, mean annual time of rise in the wetlands continued to exhibit a decreasing trend over time (Figure 2b, iv). The centroid lag, the time between the centroid of effective rainfall and the centroid of the event water level response, also became shorter over time (Figure 2c, v). However, when normalized by total annual precipitation, the decreasing trend in centroid lag was less distinct (Figure 2c, vi) as compared to the raw mean annual values. This suggests that the influence of antecedent moisture may be more important than the effects of landscape change on the centroid lag of the water level response in the connected wetlands.

4.2 | Hummock and hollow water levels

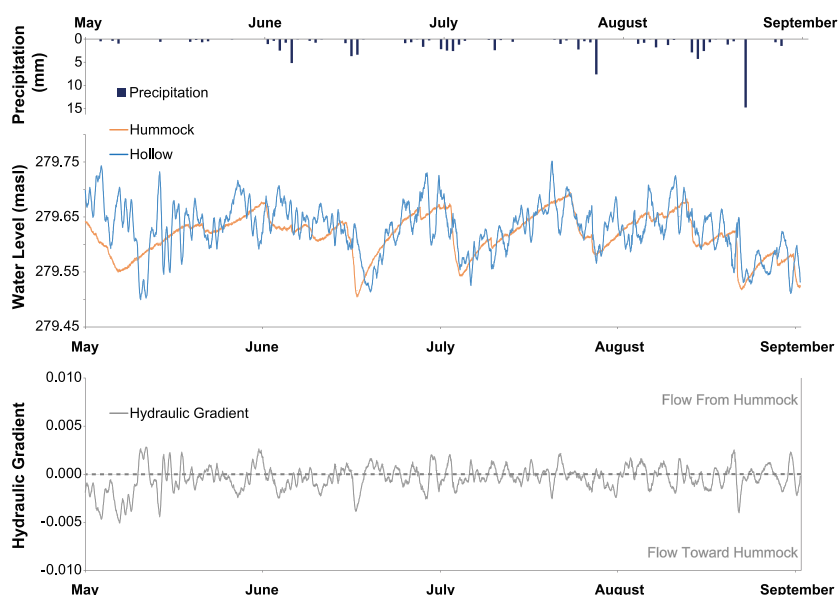
Water levels in inter-hummock hollows are variable throughout the 2020 growing season (Figure 3). The diurnal pattern throughout this 4 month period illustrates the influence of evapotranspiration on water in the hollows. The water level of the monitored hummock illustrates a comparably smoother trend, with minimal diurnal variation (Figure 3). Both the hummock and hollow water levels respond quickly to precipitation, with a slightly lagged initiation of the event response in the low-lying hollow. Throughout the course of the 2020 growing season, there are several reversals of flow between the hummock and hollow, as indicated by the hydraulic gradient (Figure 3). Early in the water level response to rainfall events, the hydraulic gradient changes direction towards the hollow from the hummock. As the events proceed, flow is reversed resulting in flow being contributed to the hummock from the hollow as water levels in the inter-hummock hollow network rise (Figure 3). The shedding of water from hummocks to hollows as rainfall events proceed is evidenced by the delay in water level rise in the hollow (Figure 3).

4.3 | Landform change

Peat plateaus are the most widely-occurring landform type in the Scotty Creek basin (40.3% in 2010 and 38.8% in 2018) and experienced the greatest change in coverage among the landform types (Table 1). Between 2010 and 2018, the percentage of peat plateau area declined by 1.4% (Table 1). The areal coverage of treed wetlands remained relatively unchanged over this period, accounting for 11.9% of the landscape in 2010 and 11.7% in 2018. The proportion of the area occupied by treed wetlands is similar to that of collapse scar wetlands, which accounted for 12.3% of the landscape in 2010 and 13.2% in 2018 (Table 1). Channel fens are the second most widely-occurring landform type in the Scotty Creek headwaters in both 2010 and 2018, representing 31.8% and 32.3%, respectively. As peat plateau areas declined, collapse scar wetlands and channel fens expanded in area. The area occupied by collapse scar wetlands increased by 0.9% between 2010 and 2018 (Table 1). The channel fens expanded by a modest increase of 0.5% over the 8 year period. Upland area remained effectively unchanged between 2010 (3.7%) and 2018 (4.0%).

In terms of the spatial distribution of the changing areal coverage of the different landform types, the overall area of peat plateaus is shrinking between 2010 and 2018 (Figure 4). In particular, this retraction of permafrost area with the loss of peat plateau coverage is occurring at the interface between peat plateaus and wetlands, specifically channel fens and collapse scar wetlands (Figure 4b,d). Expansion of collapse scar wetlands and channel fens predominantly occurred at the expense of the forested permafrost plateaus (Figure 4). Treed wetlands are primarily developing centrally within or along the periphery of wetlands with prominent connections to the basin drainage network (Figure 4). The amount of treed wetland area has increased in the four wetland sites examined here (Figure 4b,d).

FIGURE 3 Wetland water levels and precipitation (navy blue bars) for the 2020 growing season monitored in a hummock well (orange line), hollow well (blue line) and hydraulic gradient between these two wells (solid grey line). Dashed line indicates zero hydraulic gradient, with a positive gradient indicating flow from the hummock and negative gradient indicating flow towards the hummock.



Landform type	2010 Areal coverage (%)	2018 Areal coverage (%)	2018–2010 Change (%)
Peat plateau	40.3	38.8	–1.4
Treed wetland	11.9	11.7	–0.3
Collapse scar wetland	12.3	13.2	+0.9
Channel fen	31.8	32.3	+0.5
Upland	3.7	4.0	+0.3

Note: Negative percentage change values represent a loss of area between 2010 and 2018, while positive values represent a gain.

TABLE 1 Percentage of the classified 17 km² basin headwaters that is occupied by each landform type in both 2010 and 2018, as well as the percentage change in landform areal coverage from 2010 to 2018

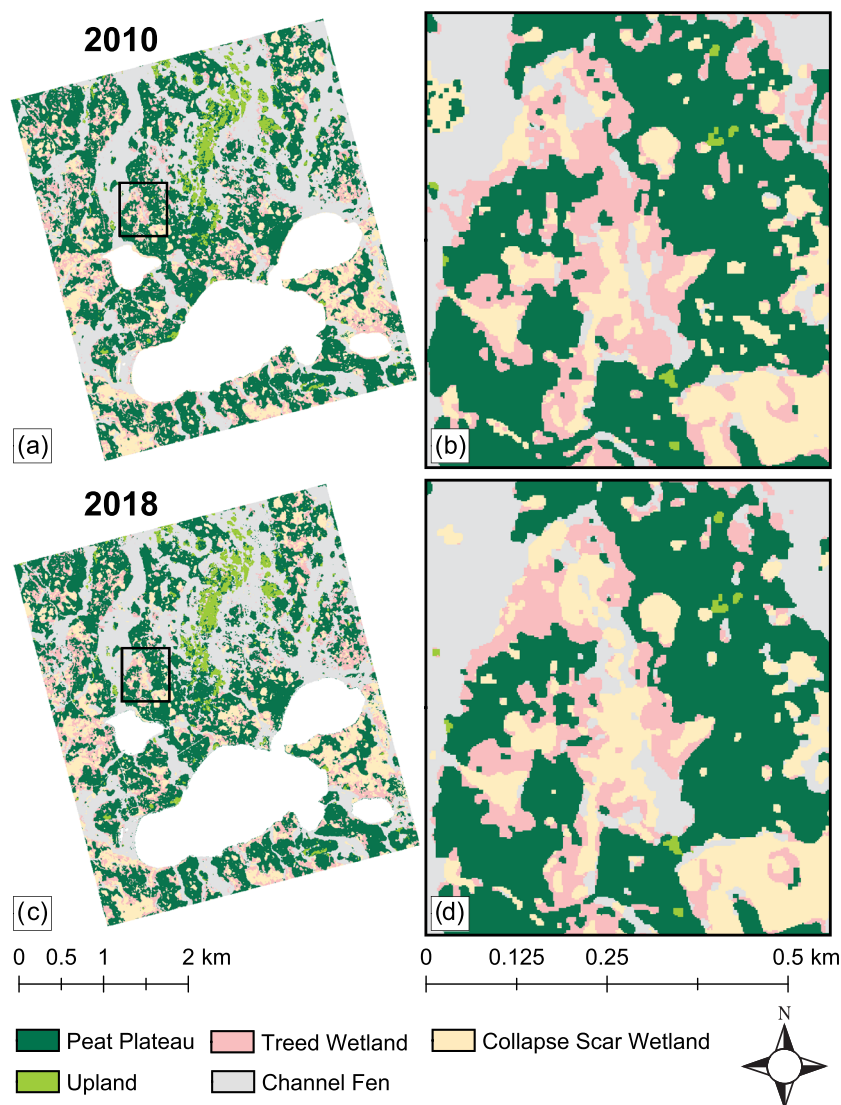


FIGURE 4 Landform classification of the (a, b) 2010 and (c, d) 2018 landscapes over approximately 17 km² of the peatland-dominated headwaters portion of the Scotty Creek basin (2010 in [a] and 2018 in [c]). The 0.6 km² study area, the focus of wetland water level monitoring, is enlarged for (b) 2010 and (d) 2018, illustrating the changing landforms over this period.

4.4 | Hummock coverage over time

The amount of area occupied by hummock terrain increased between 2010 and 2018 (Table 2). In 2010, 6.29% (37,708 m²) of the studied 0.6 km² area in the headwaters portion of the Scotty Creek basin was occupied by hummocks (Figure 5a). In 2018, 7.75% (46,500 m²) of the examined area was in the form of hummocks (Figure 5b). While the total hummock area increased, the perimeter of the

TABLE 2 Hummock characteristics over an approximately 0.6 km² portion of the Scotty Creek basin in 2010 and 2018

	2010	2018
Total hummock area (m ²)	37,708	46,500
Total hummock perimeter (m)	39,988	33,412
Hummock occurrence (%)	6.29	7.75
Hummock perimeter-to-area ratio	1.06	0.719

FIGURE 5 Hummock area (black) in (a) 2010 and (b) 2018 over the 0.6 km² study area, designated by the white border. A 2010 WorldView-2 multispectral image is the base for all panes.

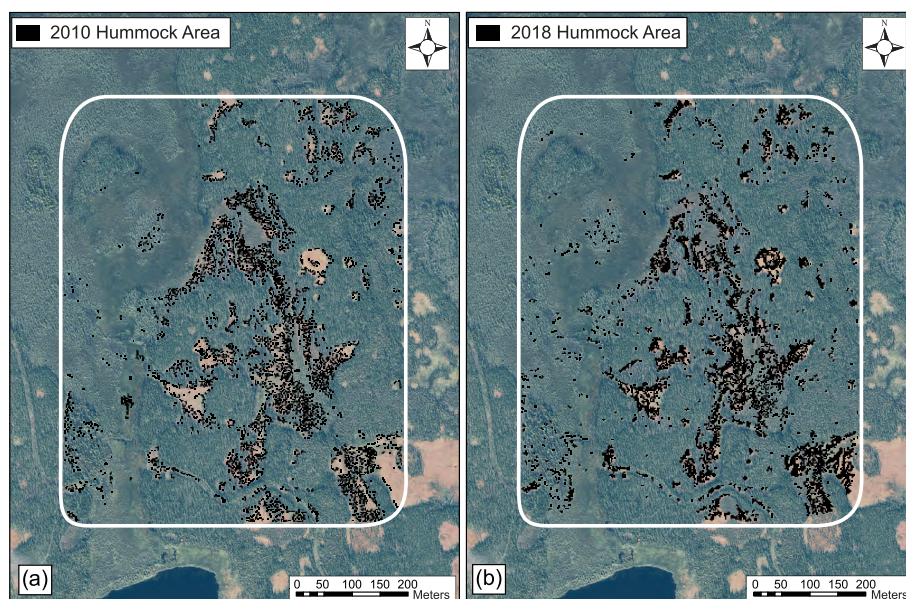


TABLE 3 Hummock characteristics in four monitored wetlands connected to the basin drainage network in 2010 and 2018

	Wetland 1		Wetland 2		Wetland 3		Wetland 4	
	2010	2018	2010	2018	2010	2018	2010	2018
Total hummock area (m ²)	2336	2252	4252	3944	1348	2308	392	480
Total hummock perimeter (m)	2516	1544	3920	2744	1652	1568	436	380
Hummock occurrence (%)	27.8	26.8	31.9	29.6	20.1	34.4	23.8	29.2
Hummock perimeter-to-area ratio	1.08	0.686	0.922	0.696	1.23	0.679	1.11	0.792

hummocks in the 0.6 km² area decreased between 2010 (39,988 m) and 2018 (33,412 m) (Table 2). Collectively, this resulted in a decrease in the hummock perimeter-to-area ratio from 1.06 in 2010 to 0.719 in 2018.

The total area occupied by hummocks increased in two of the four monitored wetlands (Table 3). In Wetland 3 and Wetland 4, total hummock area increased between 5.4% and 14.3% (Table 3). In Wetland 1 and Wetland 2, the proportion of the hummock area declined by 1.0% and 2.3%, respectively, between 2010 and 2018. Total hummock perimeter and the hummock perimeter-to-area ratios decreased between 2010 and 2018 in all four connected wetlands (Table 3).

Examination of the locations of hummock expansion and loss between 2010 and 2018 occurring in Wetland 1 and Wetland 2, which exhibited a net decrease in hummock terrain, demonstrates that the majority of hummock loss occurred along the periphery of the wetlands, in areas where the forest is re-establishing (Figures 5 and 6). The growth of trees on hummocks has the potential to obscure the identification of the underlying hummocks, therefore indicating overall hummock loss in Wetland 1 and Wetland 2 between 2010 and 2018. Expansion of hummock terrain in Wetland 1 and Wetland 2 occurred primarily in the central portion of these wetlands (Figure 6).

4.5 | Flowpath tortuosity

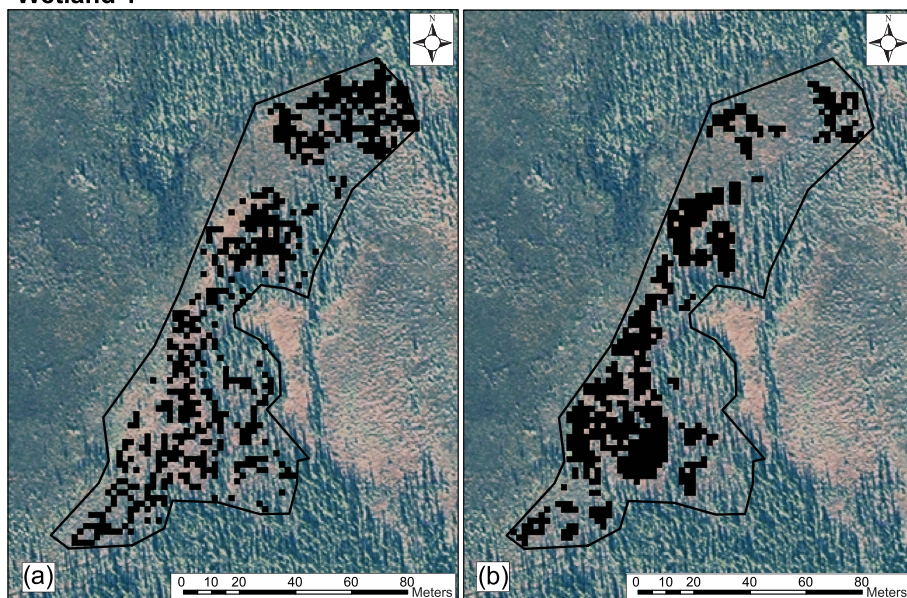
Overall, the average tortuosity of flowpaths (T_x) draining the wetlands connected to the basin drainage network increased between 2010 and 2018, with an average T_x ($n = 4$) of 1.14 in 2010 increasing to 1.20 in 2018 (Table 4). This increasing flowpath tortuosity trend was observed to varying degrees in each of the monitored connected wetlands except Wetland 2, which exhibited a decrease in T_x from 2010 (1.22) to 2018 (1.08).

5 | DISCUSSION

5.1 | Wetland transition and hummock development

Development and expansion of hydrological flowpaths connecting collapse scar wetlands to the basin drainage network allowed partial drainage of wetlands and set in motion a sequence of ecohydrological changes (Connon et al., 2014; Haynes et al., 2018, 2020). Processes are simultaneously occurring both externally to the expanding wetland area driven by permafrost thaw and internally within the wetlands resulting in the transition between wetland

Wetland 1



Wetland 2

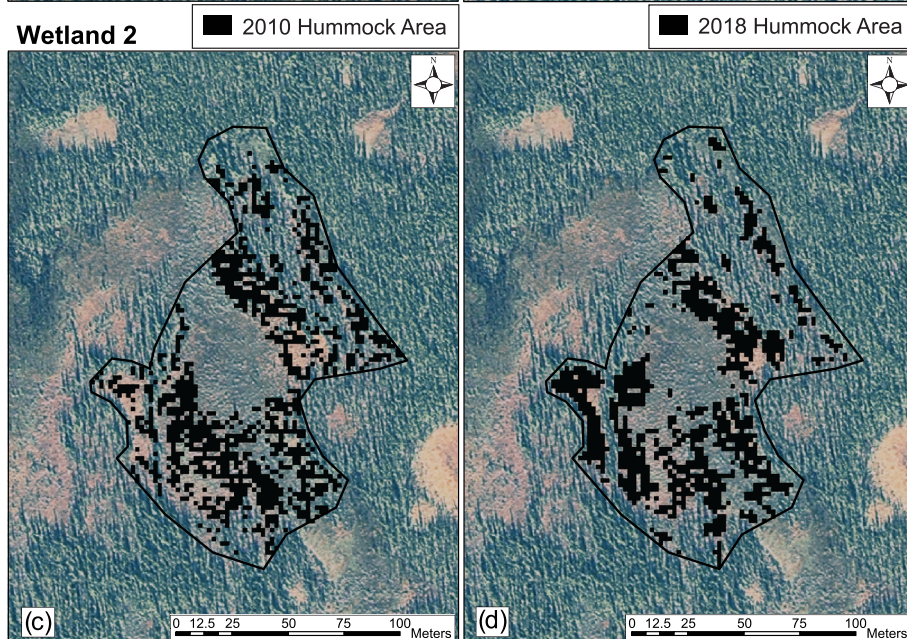


FIGURE 6 Hummock area (black) in (a, c) 2010 and (b, d) 2018 in two wetlands connected to the drainage network, (a, b) Wetland 1 and (c, d) Wetland 2, located within the broader 0.6 km² study area (Figure 1). A 2010 WorldView-2 multispectral image is the base for all panes.

TABLE 4 Average flowpath tortuosity (T_x) and standard deviation of 50 particle tracking runs for each wetland site in 2010 and 2018

Wetland site	Average flowpath tortuosity, T_x	
	2010	2018
Wetland 1	1.16 ± 0.15	1.23 ± 0.27
Wetland 2	1.22 ± 0.46	1.08 ± 0.20
Wetland 3	1.10 ± 0.08	1.39 ± 0.48
Wetland 4	1.07 ± 0.08	1.08 ± 0.06
Average	1.14	1.20

landform types (Figure 7). During the period between 2010 and 2018, the areal coverage of peat plateaus declined by 1.4%, and the area occupied by permafrost-free wetlands including collapse

scars and channel fens increased proportionately (Table 1). The permafrost thaw-driven shift from peat plateaus to open wetlands externally influenced the hydrology of the expanding wetlands. The loss of impounding permafrost resulted in the expansion of wetland area and the broadening of connections between wetlands and the drainage network, further contributing to continued partial drainage of their stored water (Figure 4). Additionally, the length of the hydrological flowpaths draining these wetlands increased, which affected the timing of discharge from individual wetlands (Figure 7).

Ongoing processes internal to the wetlands are resulting in the transition of wetland types (Figure 7). Drying of the near-surface peat following wetland ‘capture’ (Connon et al., 2014; Haynes et al., 2018) has promoted the formation of hummock–hollow microtopography

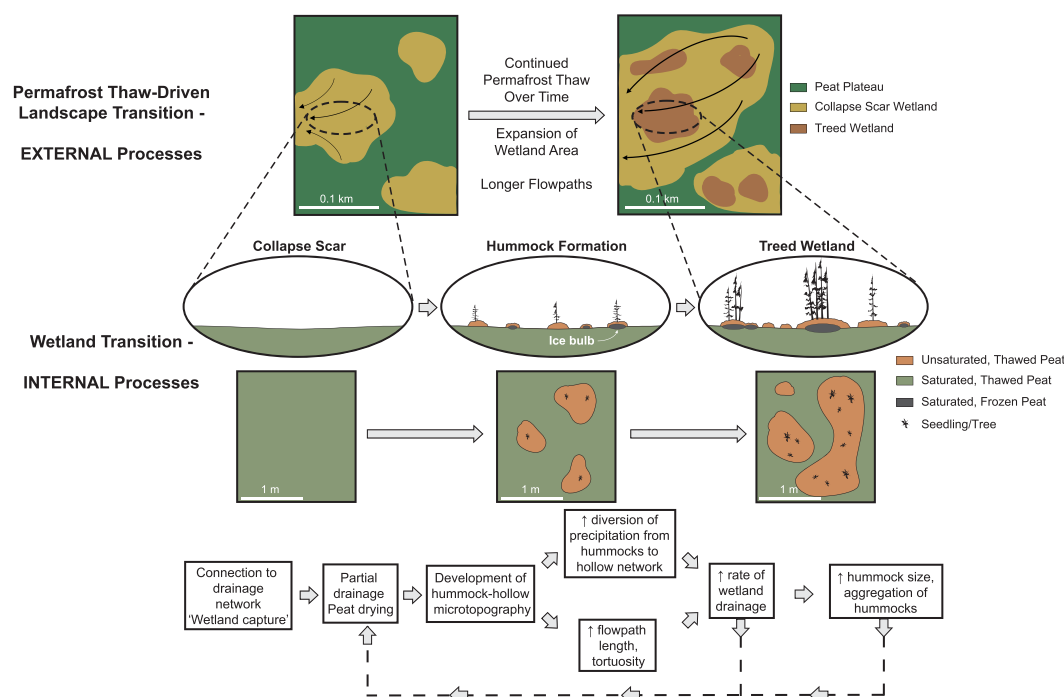


FIGURE 7 Simultaneous external and internal processes driving landscape change and wetland transition in the plateau-wetland complexes of the discontinuous permafrost environment. External processes are driven by permafrost thaw, resulting in the expansion of wetland area and the creation of longer drainage flowpaths. The changing hydrology of the expanding wetlands initiates mechanisms internal to the wetlands, resulting in wetland transition from collapse scars to treed wetlands and associated ecohydrological feedbacks. The partial drainage of wetlands connected to the drainage network promotes the development of hummock microtopography. Hummocks increase the rate of wetland drainage by diverting precipitation to the network of hollows and increasing flowpath length and tortuosity. Such ecohydrological mechanisms reinforce the partial drainage of transitioning wetlands and promote the expansion of individual hummocks and the aggregation of hummocks. Grey arrows represent direct mechanisms, while dashed lines represent potential feedbacks.

(Haynes et al., 2020), since the fast-growing hummock-forming *Sphagnum* species such as *Sphagnum magellanicum* and *S. fuscum* thrive in drier conditions (Belyea & Clymo, 2001). Between 2010 and 2018, the net proportion of hummock terrain within the study area increased from 6% to 8% (Figure 5). This process transformed open, flat collapse scar wetlands to drier hummock-occupied wetlands and as such creates the conditions needed for the subsequent, treed wetland stage (Disher et al., 2021; Haynes et al., 2020). That is, hummocks facilitate tree seedling establishment by providing physical support and suitable soil moisture (Haynes et al., 2020). The observed net increase in the total area of hummock terrain and net decrease in perimeter of individual hummocks between 2010 and 2018, and the resulting decrease in their perimeter-to-area ratio, suggests a transformation process operating at the scale of individual hummocks. Smaller individual hummocks are prevalent throughout the treed and collapse scar wetlands connected to the drainage network in 2010 (Figure 5a). In 2018, larger aggregated hummocks are located throughout the four wetlands (Figure 5b). Over this 8 year period, individual hummocks have expanded in area and have aggregated into larger hummocks capable of physically supporting one or more trees. In addition to the work of Camill (1999a) and Zoltai (1993) examining the role of hummocks in permafrost landscape change and tree colonization, the expansion and aggregation of individual hummocks to create larger

patches of hummock terrain supporting trees has previously been reported in sub-boreal, permafrost-free black ash wetlands of north-central Minnesota in the context of autogenic controls on hummock patterning and the subsequent water level dynamics (Diamond et al., 2019).

The spatial distribution of soil moisture in transition wetlands is dependent upon proximity to drainage flowpaths and areas of recent peat plateau subsidence. Peat soil moisture content in collapse scar wetlands is elevated in areas of recent peat plateau collapse, as evidenced by the prominence of *S. riparium* in these wettest sites (Gibson et al., 2018; Pelletier et al., 2017). The extent to which the wetland surface transitions from its initial state following local plateau collapse varied over a wetland. In both 2010 and 2018, hummock terrain was most well developed in central areas (Figure 5a) of the wetland since these areas are at the greatest distance from the wetland-plateau edges where ongoing permafrost thaw maintains high soil moisture contents and often saturated or even open water conditions where moats occur. For this reason, the subsequent stage of treed wetland occurs preferentially near the centre of wetlands and in areas distant from the wetland outlet (Disher et al., 2021). In areas of increased topographic variation in the form of hummocks, subsequent moisture redistribution in a positive feedback mechanism reinforces hummock development (Figure 7). Inspection of aerial imagery

collected since 1947 suggests that wetland age is greatest at the centre of wetlands and decreases with distance towards the wetland-plateau margin (Quinton et al., 2011). Therefore, the centre of wetlands has been draining for the greatest length of time, and as such, these areas are the most advanced in terms of successional stage. Ground-based observation confirms that, unlike in the central part of wetlands, wetland areas close to the plateau boundary contain both hummock-supported saplings and trees as well as sparse dying and dead trees remnant from the adjacent thawing and subsiding plateau (Haynes et al., 2020). As such, the density of tree cover near the plateau-wetland boundaries estimated from remote sensing methods could be over-estimated.

Hummocks are known to be stable and can persist in the same location over long timescales, on the order of hundreds to thousands of years (Barber, 1981). During image analysis, it was found that large trees can obscure the view of the hummocks that support them, therefore resulting in a likely underestimate of the areal coverage of hummock terrain in both 2010 and 2018 (Figures 5 and 6). The visible change in the area of hummock terrain between 2010 and 2018 indicates that individual hummocks were obscured, particularly in increasingly forested areas observed on the multispectral WorldView imagery (Figures 5 and 6). The majority of the obscured hummocks are located along the wetland-forest boundary (Figures 5 and 6).

In addition to the age of localized areas within wetlands, the time since a connection to the drainage network was developed has an impact on the successional stage of transition wetlands. The two monitored wetlands in this study that have had the longest connections to the drainage network (established just prior to 1970), Wetlands 1 and 2, demonstrated a decrease in hummock occurrence between 2010 and 2018 (Table 3). This decline in hummock coverage suggests that the tree stand supported by hummocks has matured and grown to obscure the visibility of the underlying hummocks. In contrast, Wetlands 3 and 4, which developed more recent drainage connections in the 1980s/1990s and the last decade respectively, continue to experience an expansion of hummock terrain (Table 3). Collectively, these trends may indicate that the expansion of hummocks does not occur linearly over time with landscape change and the successional stages of transition wetlands. Instead, there may be a threshold limiting the peak coverage of hummock terrain controlled by self-regulating ecohydrological feedbacks.

5.2 | Ecohydrological feedback processes

The net effect of the external and internal processes contributing to landscape change and wetland transition determines the efficiency of water movement to the channel fen drainage network. Internally, the development of hummock microtopography in transition wetlands (Haynes et al., 2020) alters drainage pathways and influences the event response. The relatively low hydraulic conductivity of the hummock-forming *Sphagnum* species and the self-regulating feedback mechanisms (Belyea & Clymo, 2001; Diamond et al., 2019) that contribute to the growth and maintenance of hummocks, including

decomposition processes, result in a lower hydraulic conductivity of the hummock peat compared with the peat in the hollows (Foster et al., 1983). Therefore, as hummock terrain spreads in wetlands, an increasing proportion of the wetland surface area is characterized by tortuous, inter-hummock flowpaths. It would therefore be anticipated that the water level recession times of such wetlands would increase as compared to those of flat, hummock-free collapse scar wetlands. The observed increase in the tortuosity of flowpaths draining wetlands indicates that the pathway for runoff is more tortuous due to the obstruction posed by hummocks (Table 4). However, this increase in flowpath tortuosity was not accompanied by longer water level recessions following precipitation events (Figure 2a).

The shorter observed wetland water level recession times are likely a function of the role the hummocks directly play in the conversion of precipitation to runoff. These low hydraulic conductivity landscape features (Belyea & Clymo, 2001) redirect water received from rainfall to adjacent, low-lying inter-hummock hollow areas, the peat soils of which are of higher hydraulic conductivity. The shedding of precipitation from hummocks to hollows is evidenced by the transition of the hydraulic gradient from hummocks early on during the course of a precipitation event to hollows as the event progresses and flows are subsequently reversed as hollow water levels rise (Figure 3). As water levels rise in the inter-hummock hollows, the rate of water movement would be expected to increase, as the permeability and hydraulic conductivity of near-surface peat soils and living *Sphagnum* moss in hollows are greater than deeper within the peat profile (Quinton et al., 2008). Despite the increase in flowpath tortuosity with the development of hummock terrain (Table 4), the hydraulic relationship between hummocks and inter-hummock hollows drove a faster water level response to rainfall (Figure 2b, iii). The increasing size of individual hummocks and the expansion of hummock terrain increased the drainage efficiency of wetlands connected to the drainage network, as observed with the declining recession constants (Figure 2a, i) over time. When normalized by annual precipitation, the long-term patterns in wetland water level recession constants (Figure 2a, ii), time of rise (Figure 2b, iv) and, to a lesser extent, centroid lag (Figure 2c, vi) continued to exhibit a decreasing trend. This supports the concept that the changes in hydraulic event response and water level recession constants are not driven by inter-annual changes in precipitation throughout the monitoring period, but rather the internal and external processes involved with wetland transition and landscape evolution initiated by permafrost thaw. Efficient runoff of rainfall from these transitioning wetlands will reduce the amount of standing water available for evapotranspiration. This reduction in water storage will likely further be impacted by the return of tree canopy in the form of hummock-supported treed wetlands, as transpiration from seedlings and growing trees feedbacks to alter the cycling of water in these changing systems.

The observed quicker wetland water level recession over time is likely also externally influenced by the continued landscape change resulting from permafrost thaw (Figure 7). In the plateau-wetland complexes of the Taiga Plains ecoregion, wetlands are expanding at the expense of forested peat plateaus as permafrost bodies warm and

degrade (Carpino et al., 2021). As individual wetlands expand and the overall area of wetlands increases concomitantly with peat plateau contraction, the length of hydrological flowpaths draining connected wetlands increases (Figure 7). Additionally, the broadening of connections between wetlands and the drainage network with ongoing permafrost thaw promotes continued drainage of stored water (Connon et al., 2014; Haynes et al., 2018) and quicker discharge of both event and pre-event water from the wetlands. Collapse scar wetlands formed following the subsidence of peat plateaus are irregularly shaped. The evolving shape of transition wetlands likely impacts the hydrology of these wetlands (Morris et al., 2011), as such changes increase the precipitation volume received with the increased wetland surface area and alter the hydraulic gradient. Parsing out the potential impacts of the changing geometry of collapse scar wetlands with continued permafrost thaw and wetland transition would provide a greater understanding of the impacts of landscape change on the routing and drainage efficiency of water in the dynamic discontinuous permafrost zone.

In addition to the size and shape of the expanding wetlands, the spatial distribution and configuration of developing hummocks will likely impact the hydrological processes governing these systems and the feedback mechanisms associated with continued landscape change. Hummocks configured in a linear ridge would create a greater impedance to flow than an identically-sized group of hummocks distributed in a randomized pattern (Belyea & Baird, 2006). As wetlands continue to transition with ongoing and accelerating permafrost thaw, the resultant ecohydrological feedbacks will likely yield self-organization of the spatial patterning of hummock microforms (Belyea & Baird, 2006; Eppinga et al., 2009). Therefore, apparently randomized distributions of hummocks developing in transition wetlands may self-organize to form distinct patterning over time as treed wetlands mature and continue to contribute stored water to discharge. Given the ability of hummocks to shed precipitation to surrounding hollows and impact the routing of water flows, the spatial distribution, in addition to total area, of hummock terrain may affect the ecohydrological transition of thawing discontinuous permafrost landscapes. The presence of hummock terrain and their role in supporting the return of tree cover to the open wetlands of the subarctic may ensure the resilience of these forested ecosystems despite the loss of permafrost. Further investigation of the spatial patterning of developing hummock terrain will likely have important implications for not only the small-scale ecohydrology of transition wetlands but also the broader long-term sustainability of freshwater resources in the plateau-wetland complexes of the discontinuous permafrost zone.

ACKNOWLEDGEMENTS

We wish to thank the Dehcho First Nations, including the Liidlii Kue First Nation, Jean Marie River First Nation and Sambaa K'e First Nation, for their support and acknowledge that the Scotty Creek Research Station is located on Treaty 11 land. We acknowledge funding support from ArcticNet for the Dehcho Collaborative on Permafrost as well as a Natural Sciences and Engineering Research Council of Canada (NSERC) Discovery Grant to W.L.Q. We appreciate the

assistance of W. Tang in parameterizing HydRun and M. Mack in using MATLAB. We thank M. Auclair and I. Thompson for assistance in field data collection. The 2010 and 2018 Light Detection and Ranging (LiDAR) data were provided by C. Hopkinson and L. Chasmer, University of Lethbridge. We thank those who provided a constructive review of this manuscript.

DATA AVAILABILITY STATEMENT

The data that support the findings of this study are available from the corresponding author upon reasonable request.

ORCID

Kristine M. Haynes  <https://orcid.org/0000-0002-9529-4640>

REFERENCES

- Barber, K. E. (1981). *Peat stratigraphy and climatic change: A palaeoecological test of the theory of cyclic bog regeneration*. Balkema.
- Belyea, L. R., & Baird, A. J. (2006). Beyond “the limits to peat bog growth”: Cross-scale feedback in peatland development. *Ecological Monographs*, 76, 299–322. [https://doi.org/10.1890/0012-9615\(2006\)076%5B0299:BTLPB%5D2.0.CO;2](https://doi.org/10.1890/0012-9615(2006)076%5B0299:BTLPB%5D2.0.CO;2)
- Belyea, L. R., & Clymo, R. S. (2001). Feedback control of the rate of peat formation. *Proceedings of the Royal Society of London B*, 268, 1315–1321. <https://doi.org/10.1098/rspb.2001.1665>
- Camill, P. (1999a). Peat accumulation and succession following permafrost thaw in the boreal peatlands of Manitoba, Canada. *Ecoscience*, 6, 592–602. <https://doi.org/10.1080/11956860.1999.11682561>
- Camill, P. (1999b). Patterns of boreal permafrost peatland vegetation across environmental gradients sensitive to climate warming. *Canadian Journal of Botany*, 77(5), 721–733. <https://doi.org/10.1139/b99-008>
- Carpino, O. A., Haynes, K. M., Connon, R., Craig, J., Devoie, É., & Quinton, W. L. (2021). Long-term climate-influenced land cover change in discontinuous permafrost peatland complexes. *Hydrology and Earth System Sciences*, 25, 3301–3317. <https://doi.org/10.5194/hess-2020-411>
- Chasmer, L., & Hopkinson, C. (2017). Threshold loss of discontinuous permafrost and landscape evolution. *Global Change Biology*, 23, 2672–2686. <https://doi.org/10.1111/gcb.13537>
- Chasmer, L., Hopkinson, C., Quinton, W., Veness, T., & Baltzer, J. (2014). A decision-tree classification for low-lying complex land cover types within the zone of discontinuous permafrost. *Remote Sensing of Environment*, 143, 73–84. <https://doi.org/10.1016/j.rse.2013.12.016>
- Chasmer, L., Quinton, W., Hopkinson, C., Petrone, R., & Whittington, P. (2011). Vegetation canopy and radiation controls on permafrost plateau evolution within the discontinuous permafrost zone, Northwest Territories, Canada. *Permafrost and Periglacial Processes*, 22, 199–213. <https://doi.org/10.1002/ppp.724>
- Connon, R. F., Quinton, W. L., Craig, J. R., & Hayashi, M. (2014). Changing hydrologic connectivity due to permafrost thaw in the lower Liard River valley, NWT, Canada. *Hydrological Processes*, 28, 4163–4178. <https://doi.org/10.1002/hyp.10206>
- Diamond, J. S., McLaughlin, D. L., Slesak, R. A., & Stovall, A. (2019). Pattern and structure of microtopography implies autogenic origins in forested wetlands. *Hydrology and Earth System Sciences*, 23, 5069–5088. <https://doi.org/10.5194/hess-23-5069-2019>
- Disher, B. S., Connon, R. F., Haynes, K. M., Hopkinson, C., & Quinton, W. L. (2021). The hydrology of treed wetlands in thawing discontinuous permafrost regions. *Ecohydrology*, 14(5), e2296. <https://doi.org/10.1002/eco.2296>
- Eppinga, M. B., Rietkerk, M., Wassen, M. J., & De Ruiter, P. C. (2009). Linking habitat modification to catastrophic shifts and vegetation patterns

- in bogs. *Plant Ecology*, 200, 53–68. <https://doi.org/10.1007/s11258-007-9309-6>
- Foster, D. R., King, G. A., Glaser, P. H., & Wright, H. E. Jr. (1983). Origin of string patterns in boreal peatlands. *Nature*, 306, 256–258. <https://doi.org/10.1038/306256a0>
- Garon-Labrecque, M.-È., Léveillé-Bourret, É., Higgins, K., & Sonnentag, O. (2015). Additions to the boreal flora of the Northwest Territories with a preliminary vascular flora of Scotty Creek. *Canadian Field Naturalist*, 129, 349–367. <https://doi.org/10.22621/cfn.v129i4.1757>
- Gibson, C. M., Chasmer, L. E., Thompson, D. K., Quinton, W. L., Flannigan, M. D., & Olefeldt, D. (2018). Wildfire as a major driver of recent permafrost thaw in boreal peatlands. *Nature Communications*, 9(1), 3041. <https://doi.org/10.1038/s41467-018-05457-1>
- Hayashi, M., Quinton, W. L., Pietroniro, A., & Gibson, J. J. (2004). Hydrologic functions of wetlands in a discontinuous permafrost basin indicated by isotopic and chemical signatures. *Journal of Hydrology*, 296(1–4), 81–97. <https://doi.org/10.1016/j.jhydrol.2004.03.020>
- Haynes, K. M., Connon, R. F., & Quinton, W. L. (2018). Permafrost thaw induced drying of wetlands at Scotty Creek, NWT, Canada. *Environmental Research Letters*, 13(11), 114001. <https://doi.org/10.1088/1748-9326/aae46c>
- Haynes, K. M., Smart, J., Disher, B., Carpino, O., & Quinton, W. L. (2020). The role of hummocks in re-establishing black spruce forest following permafrost thaw. *Ecohydrology*, 14(3), e2273. <https://doi.org/10.1002/eco.2273>
- Islam, M. A., & Macdonald, S. E. (2004). Ecophysiological adaptations of black spruce (*Picea mariana*) and tamarack (*Larix laricina*) seedlings to flooding. *Trees - Structure and Function*, 18, 35–42. <https://doi.org/10.1007/s00468-003-0276-9>
- Jorgenson, M. T., & Osterkamp, T. E. (2005). Response of boreal ecosystems to varying modes of permafrost degradation. *Canadian Journal of Forest Research*, 35, 2100–2111. <https://doi.org/10.1139/x05-153>
- Jorgenson, M. T., Racine, C. H., Walters, J. C., & Osterkamp, T. E. (2001). Permafrost degradation and ecological changes associated with a warming climate in central Alaska. *Climatic Change*, 48, 551–579. <https://doi.org/10.1023/A:1005667424292>
- Lara, M. J., Genet, H., McGuire, A. D., Euskirchen, E. S., Zhang, Y., Brown, D. R. N., Jorgenson, M. T., Romanovsky, V., Breen, A., & Bolton, W. R. (2016). Thermokarst rates intensify due to climate change and forest fragmentation in an Alaskan boreal forest lowland. *Global Change Biology*, 22, 816–829. <https://doi.org/10.1111/gcb.13124>
- Lyon, S. W., & Destouni, G. (2010). Changes in catchment-scale recession flow properties in response to permafrost thawing in the Yukon River basin. *International Journal of Climatology*, 30, 2138–2145. <https://doi.org/10.1002/joc.1993>
- Lyon, S. W., Destouni, G., Giesler, R., Humborg, C., Mörrh, M., Seiberet, J., Karlsson, J., & Troch, P. A. (2009). Estimation of permafrost thawing rates in a sub-arctic catchment using recession flow analysis. *Hydrology and Earth System Sciences*, 13, 595–604. <https://doi.org/10.5194/hess-13-595-2009>
- McClymont, A. F., Hayashi, M., Bentley, L. R., & Christensen, B. S. (2013). Geophysical imaging and thermal modeling of subsurface morphology and thaw evolution of discontinuous permafrost. *Journal of Geophysical Research*, 118(3), 1826–1837. <https://doi.org/10.1002/jgrf.20114>
- Morris, P. J., Belyea, L. R., & Baird, A. J. (2011). Ecohydrological feedbacks in peatland development: A theoretical modelling study. *Journal of Ecology*, 99(5), 1190–1201. <https://doi.org/10.1111/j.1365-2745.2011.01842.x>
- Pelletier, N., Talbot, J., Olefeldt, D., Turetsky, M., Blodau, C., Sonnentag, O., & Quinton, W. L. (2017). Influence of Holocene permafrost aggradation and thaw on the paleoecology and carbon storage of a peatland complex in northwestern Canada. *The Holocene*, 27, 1391–1405. <https://doi.org/10.1177/0959683617693899>
- Quinton, W., Berg, A., Braverman, M., Carpino, O., Chasmer, L., Connon, R., Craig, J., Devoie, É., Hayashi, M., Haynes, K., Olefeldt, D., Pietroniro, A., Rezanezhad, F., Schincariol, R., & Sonnentag, O. (2019). A synthesis of three decades of hydrological research at Scotty Creek, NWT, Canada. *Hydrology and Earth System Sciences*, 23, 1–25. <https://doi.org/10.5194/hess-23-1-2019>
- Quinton, W. L., & Baltzer, J. L. (2013). The active-layer hydrology of a peat plateau with thawing permafrost (Scotty Creek, Canada). *Hydrogeology Journal*, 21(1), 201–220. <https://doi.org/10.1007/s10040-012-0935-2>
- Quinton, W. L., & Marsh, P. (1998). The influence of mineral earth hummocks on subsurface drainage in the continuous permafrost zone. *Permafrost and Periglacial Processes*, 9, 213–228.
- Quinton, W. L., Hayashi, M., & Carey, S. K. (2008). Peat hydraulic conductivity in cold regions and its relation to pore size and geometry. *Hydrological Processes*, 22, 2829–2837. <https://doi.org/10.1002/hyp.7027>
- Quinton, W. L., Hayashi, M., & Chasmer, L. E. (2011). Permafrost thaw-induced land-cover change in the Canadian subarctic: Implications for water resources. *Hydrological Processes*, 25(1), 152–158. <https://doi.org/10.1002/hyp.7894>
- Quinton, W. L., Hayashi, M., & Pietroniro, A. (2003). Connectivity and storage functions of channel fens and flat bogs in northern basins. *Hydrological Processes*, 17(18), 3665–3684. <https://doi.org/10.1002/hyp.1369>
- Richter-Menge, J., Overland, J. E., Mathis, J. T., & Osborne, E. (Eds.). (2017). Arctic report card. <http://www.arctic.noaa.gov/Report-Card>
- St. Jacques, J. M., & Sauchyn, D. J. (2009). Increasing winter baseflow and mean annual streamflow from possible permafrost thawing in the Northwest Territories, Canada. *Geophysical Research Letters*, 36, L01401. <https://doi.org/10.1029/2008GL035822>
- Tang, W., & Carey, S. K. (2017). HydRun: A MATLAB toolbox for rainfall-runoff analysis. *Hydrological Processes*, 31, 2670–2682. <https://doi.org/10.1002/hyp.11185>
- Waddington, J. M., Morris, P. J., Kettridge, N., Granath, G., Thompson, D. K., & Moore, P. A. (2015). Hydrological feedbacks in northern peatlands. *Ecohydrology*, 8, 113–127. <https://doi.org/10.1002/eco.1493>
- Wright, N., Hayashi, M., & Quinton, W. L. (2009). Spatial and temporal variations in active layer thawing and their implication on runoff generation in peat-covered permafrost terrain. *Water Resources Research*, 45(5), W05414. <https://doi.org/10.1029/2008WR006880>
- Zoltai, S. C. (1993). Cyclic development of permafrost in the peatlands of northwestern Alberta, Canada. *Arctic and Alpine Research*, 25, 240–246. <https://doi.org/10.1080/00040851.1993.12003011>

How to cite this article: Haynes, K. M., Frederick, I., Disher, B., Carpino, O., & Quinton, W. L. (2022). Long-term trends in wetland event response with permafrost thaw-induced landscape transition and hummock development. *Ecohydrology*, e2515. <https://doi.org/10.1002/eco.2515>